Effect of Lattice Vibrations in a Multiple-Scattering Description of Low-Energy Electron Diffraction. II. Double-Diffraction Analysis of the Elastic Scattering Cross Section*

G. E. LARAMORE† AND C. B. DUKE
Department of Physics, Materials Research Laboratory and Coordinated Science Laboratory, University of Illinois, Urbana-Champaign, Illinois 61801

(Received 19 June 1970)

The evaluation of the elastic scattering differential cross section of electron scattering from a planar surface of a vibrating lattice is reduced to the solution of a set of coupled algebraic equations for the associated scattering amplitude. This reduction is valid both for overlapping potentials (thus removing the restriction of previous analyses to muffin-tin potentials) and for the nonspherical potentials associated with ion cores at solid surfaces. The algebraic equations are solved using a double-diffraction analysis of the inelastic-collision model. Surface scatterers are taken to be geometrically equivalent but electronically and vibronically inequivalent to those in the bulk. A Debye model is used to describe the phonon spectrum of the solid. Numerical results are presented for a hypothetical fcc metal with the lattice parameters of aluminum. Thermal expansion alters the energies of peaks in the elastic intensity profiles (I–V curves), whereas the thermal vibration of the ion cores alters the intensities of the peaks. The temperature dependence of the peak heights can be described by the kinematic model in which it is attributed to the Debye-Waller factor associated with an "effective" Debye temperature. However, the multiple scattering of the electron from the lattice causes these "effective" Debye temperatures to be related to the parameters of the model (e.g., bulk and surface electron–ion-core scattering phase shifts, the inelastic-collision mean free path, bulk- and surface-model Debye temperatures) in a complicated fashion. Although the trends evident in the dependence of the effective Debye temperature on the model parameters can be rendered plausible, it appears almost impossible to extract from a kinematical model reliable quantitative information about the average thermal displacements of the surface and bulk ion cores.

I. INTRODUCTION

In the past two years, rapid progress has been achieved in constructing an adequate theory of elastic low-energy electron diffraction (LEED) by virtue of the recognition that strong inelastic-collision damping as well as strong electron–ion-core scattering is an important ingredient in such a theory.[1–6] The microscopic origin of most of this damping is thought to be large-energy ($\Delta E \gtrsim 2$ eV) electron-loss processes associated with interband transitions and plasmon excitation in the solid.[1,7–9] Therefore, one direction of development of the present theory is the explicit description of the coupling between the elastic and inelastic scattering channels for the incident electron.[8–11] However, in this and a previous paper,[12] we have developed the theory in a second direction, by extending it to incorporate a description of electron scattering from the low-energy ($\Delta E \sim 10$ meV) atomistic collective excitations of the lattice (phonons) within the framework of the inelastic-collision-model description[1,2–5] of strong electron–ion-core elastic scattering and strong inelastic-collision damping via large-energy electronic excitations of the solid.

The study of the influence of lattice vibrations on the scattering of x rays[13] and neutrons[14] is an old and venerable topic. However, the interactions of x rays and neutrons with solids differ in one crucial respect from those of electrons with solids: They are sufficiently weak that multiple-scattering effects usually are unimportant. This fact has the consequence that linear-response theory describes the interaction process. The extensive theories of x-ray and neutron diffraction are based on this result. Because of this historical background, it is natural that early models of low-energy electron scattering from phonons[15,16] and magnons[17,18] also were based on linear-response theory. We refer to such models as "kinematical" in nature (following the nomenclature for elastic LEED from rigid lattices[1]) and note that they have been used extensively in analyzing the available experimental data on the temperature dependence and (angular) line shapes of LEED differential cross sections.[19,20] Unfortunately, similar analyses of elastic electron scattering from a rigid lattice utterly fail to describe analogous features of the experimental data.[1–6,21(a)] They also seem to fail in describing thermal effects.[21(b)] Consequently in our first paper[12] (hereafter referred to as DL) we formally extended the theory to describe multiple-interaction processes in both the elastic and inelastic channels.

In this paper we consider only the influence of the lattice vibrations on the elastic scattering of the incident electron by the solid. As noted in DL, the major vehicle whereby this influence is exerted is the renormalization of the electron–ion-core vertices by the Debye-Waller factor. The content of this paper consists of first reducing to algebraic form the integral equations describing the multiple scattering of the electron from this renormalized potential, and then solving the resulting algebraic equations in the double-diffraction approximation.[4] Our principal result is the discouraging observation that the extraction from experimental data of quantitative information on the mean displacement of surface atoms is not possible at the present time because of the sensitivity of the model predictions on the (largely unknown) parameters de-

scribing the electron–ion-core scattering and inelastic-collision damping in the surface region. This fact does not seem to have been fully appreciated in experimental data analyses.[22–26] In this context, it is worth recalling[3,5] that our double-diffraction analysis is as nearly a "kinematical" calculation as one can sensibly perform in describing LEED from solids.[3–5] The use of an improved description of higher-order multiple scattering[5,6] doubtless will complicate the situation still further, although we anticipate[5] that for the values of the parameters used in our numerical calculations, the alterations in the results of these calculations will be small.

In Sec. II we review the integral equations derived in DL, make a partial-wave decomposition, and change these integral equations into a set of algebraic equations *without* restricting the lattice site potential to the muffin-tin form used by Beeby.[27] In Sec. III we describe the model we shall use for our numerical analysis of the equations of Sec. II and in Sec. IV we give the results of this analysis. We display curves showing the effect of temperature upon the elastic energy profiles and analyze our results so as to obtain an effective Debye temperature for each peak. Those who are interested primarily in our results and not in the details of the theory may skip directly to Sec. IV. Finally, in Sec. V we summarize our conclusions.

II. REDUCTION OF INTEGRAL EQUATIONS FOR SCATTERING AMPLITUDE TO ALGEBRAIC FORM

In DL the dominant diagrams contributing to the elastic scattering cross section were summed. The resulting expression for the cross section is given by the following equations:

$$d^2\sigma/dE\,d\Omega\,|_{\mathbf{k}_i\to\mathbf{k}_f\ \mathrm{elas}} = [m^2/(2\pi\hbar^2)^2]\delta(E_f-E_i)\,|\,I(\mathbf{k}_f,\mathbf{k}_i;E_i)\,|^2, \quad (1)$$

$$I(\mathbf{k}_f,\mathbf{k}_i;E_i) = N_{||}\sum_\lambda\sum_{\mathbf{g}}\exp[-i(k_{f\perp}-k_{i\perp})d_\lambda - i\mathbf{g}\cdot\mathbf{a}] \times T_\lambda(\mathbf{k}_f,\mathbf{k}_i;E_i)\delta(\mathbf{k}_{f||}-\mathbf{k}_{i||}-\mathbf{g}), \quad (2)$$

$$T_\lambda(\mathbf{k}_f,\mathbf{k}_i;E_i) = \tau_\lambda(\mathbf{k}_f,\mathbf{k}_i;E_i) + \sum_{\mathbf{k}}\sum_{\lambda_1\neq\lambda}\tau_\lambda(\mathbf{k}_f,\mathbf{k};E_i) \times G^{\lambda\lambda_1}(\mathbf{k},\mathbf{k}_i;E_i)T_{\lambda_1}(\mathbf{k},\mathbf{k}_i;E_i), \quad (3)$$

$$\tau_\lambda(\mathbf{k}_f,\mathbf{k}_i;E_i) = b_\lambda(\mathbf{k}_f,\mathbf{k}_i;E_i) + \sum_{\mathbf{k}} b_\lambda(\mathbf{k}_f,\mathbf{k};E_i)G^{\mathrm{sp}}(\mathbf{k},\mathbf{k}_i;E_i)\tau_\lambda(\mathbf{k},\mathbf{k}_i;E_i), \quad (4)$$

$$b_\lambda(\mathbf{k}_f,\mathbf{k}_i;E_i) = \exp[-W_\lambda(\mathbf{k}_f-\mathbf{k}_i)]t_\lambda(\mathbf{k}_f,\mathbf{k}_i;E_i), \quad (5)$$

$$t_\lambda(\mathbf{k}_f,\mathbf{k}_i;E_i) = v_\lambda(\mathbf{k}_f-\mathbf{k}_i) + \sum_{\mathbf{k}} v_\lambda(\mathbf{k}_f-\mathbf{k})G(\mathbf{k};E_i)t_\lambda(\mathbf{k},\mathbf{k}_i;E_i). \quad (6)$$

In the above equations $v_\lambda(\mathbf{q})$ is the qth Fourier component of the interaction between the electron and an ion located in the λth plane from the surface. The quantity

$$G(\mathbf{k};E_i) = [E_i-\hbar^2k^2/2m-\Sigma(\mathbf{k},E_i)]^{-1} \quad (7)$$

is the propagator that describes the motion of the incident electron through the conduction electrons of the metal. We also used the subplane and interlayer propagators defined by

$$G^{\mathrm{sp}}(\mathbf{k},\mathbf{k}_i;E_i) = G(\mathbf{k},E_i)\sum_{\mathbf{P}\neq0}\exp[-i(\mathbf{k}_{||}-\mathbf{k}_{i||})\cdot\mathbf{P}], \quad (8)$$

$$G^{\lambda\lambda_1}(\mathbf{k},\mathbf{k}_i;E_i) = G(\mathbf{k},E_i)\sum_{\mathbf{P}}\exp\{-i[\mathbf{k}_{||}-\mathbf{k}_{i||}]\cdot[\mathbf{P}+\mathbf{a}(\lambda_1-\lambda)]-i(k_\perp-k_{i\perp})\times(d_{\lambda_1}-d_\lambda)\}. \quad (9)$$

The effective site scattering vertices given in Eq. (5) are the rigid-site scattering vertices t_λ renormalized by the Debye-Waller factors,

$$W_\lambda(\mathbf{k}_f-\mathbf{k}_i) = \tfrac{1}{2}(k_f-k_i)^\alpha\langle u_{l,\lambda}{}^\alpha(0)u_{l,\lambda}{}^\beta(0)\rangle_T(k_f-k_i)^\beta. \quad (10)$$

In Eq. (7) $\Sigma(\mathbf{k},E_i)$ is a complex electronic self-energy[1] which describes the interaction between the electrons of the beam and the conduction electrons of the solid.

In obtaining the above equations we have made the following assumptions[1,3–5]:

(a) The solid is taken to consist of subplanes of ion cores parallel to the surface. Each subplane consists of the same two-dimensional Bravais lattice. The quantity $\mathbf{P}$ is a vector in the subplane and $\mathbf{g}$ is a vector in the reciprocal lattice of the subplane.

(b) A particular value of the index λ denotes a given subplane. All scatterers in a given subplane are taken to be identical. The quantity $u_{l,\lambda}{}^\alpha(0)$ is the αth component of the displacement from equilibrium of the lth atom in the λth subplane. We adopt the convention of summing over repeated Cartesian indices.

(c) The quantity $\mathbf{a}$ is a vector denoting the shift in the positions of the center atom between successive subplanes, and d_λ is the perpendicular distance of the λth subplane from the surface (i.e., $d_0\equiv0$).

For convenience in the numerical calculations, we shall assume that the electronic self-energy depends only on the energy of the electron and not on its momentum. Hence we write

$$G(\mathbf{k},E) = \left(E-\frac{\hbar^2k^2}{2m}-\Sigma(E)\right)^{-1} = \frac{2m/\hbar^2}{k^2(E)-k^2}, \quad (11)$$

where

$$\hbar^2k^2(E)/2m \equiv E-\Sigma(E). \quad (12)$$

We also shall use the fact that

$$G(\mathbf{k},E) = G(\,|\,\mathbf{k}\,|,E) \quad (13)$$

in making our partial-wave decompositions.

As a notational convenience let us define

$$Y_{l,m}(\Omega)\equiv Y_L(\Omega), \quad (14)$$

where the $Y_{l,m}(\Omega)$ are the familiar spherical harmonic

functions,[28] and

$$\sum_L \equiv \sum_l \sum_{m=-l}^{l}. \tag{15}$$

If we assume that the interaction between the incident electron and an ion core in the solid is spherically symmetric in coordinate space, then

$$v_\lambda(\mathbf{k}_1-\mathbf{k}_2)=v_\lambda(\,|\mathbf{k}_1-\mathbf{k}_2|\,). \tag{16}$$

The reduction of Eqs. (3)–(6) to algebraic form is accomplished by partial-wave expansions. Therefore let us begin this reduction by reviewing, in a convenient notation, the well-known partial-wave expansion of the single-site t-matrix equation (6) (as all of the vertices are characterized by the same energy E_i, we drop this designation and set $E\equiv E_i$):

$$\begin{aligned} t_\lambda(\mathbf{k}_f,\mathbf{k}_i) &= \sum_L t_\lambda^L(k_f,k_i)\,Y_L^*(\Omega_F)\,Y_L(\Omega_i) \\ &= \sum_L v_\lambda^L(k_f,k_i)\,Y_L^*(\Omega_f)\,Y_L(\Omega_i) \\ &+ \sum_{\mathbf{k}}\sum_L\sum_{L_1} v_\lambda^L(k_f,k)\,Y_L^*(\Omega_f)\,Y_L(\Omega)G(k,E) \\ &\times Y_{L_1}^*(\Omega)\,Y_{L_1}(\Omega_i)\,t_\lambda^{L_1}(k,k_i). \end{aligned} \tag{17}$$

We always take the continuum limit with regard to the plane-wave states of the electron, i.e.,

$$\sum_{\mathbf{k}} \to \int (dk)/(2\pi)^3. \tag{18}$$

From the orthogonality property of the spherical harmonics

$$\int (d\Omega)\,Y_L(\Omega)\,Y_{L_1}^*(\Omega)=\delta_{L,L_1}, \tag{19}$$

we obtain

$$\begin{aligned} T_\lambda^L(k_f,k_i) &= v_\lambda^L(k_f,k_i) \\ &+ \frac{1}{(2\pi)^3}\int_0^\infty dk k^2 v_\lambda^L(k_f,k)G(k,E)t_\lambda^L(k,k_i). \end{aligned} \tag{20}$$

However, $v_\lambda(\,|\mathbf{k}_1-\mathbf{k}_2|\,)$ can depend only on $|\mathbf{k}_1|$, $|\mathbf{k}_2|$, and $\cos\theta$, where θ is the angle between $\mathbf{k}_1$ and $\mathbf{k}_2$. Hence, a direct expansion of $v_\lambda(\,|\mathbf{k}_1-\mathbf{k}_2|\,)$ yields

$$\begin{aligned} &v_\lambda(\,|\mathbf{k}_1-\mathbf{k}_2|\,) \\ &= \sum_{n=0}^{\infty}\left(\frac{\partial^n}{-\partial(2k_1k_2\cos\theta)^n}\,v_\lambda(k_1,k_2;\cos\theta)\right)_{2k_1k_2\cos\theta=0} \\ &\times \frac{(2k_1k_2\cos\theta)^n}{n!}. \end{aligned} \tag{21}$$

Since

$$[\partial n/\partial(2k_1k_2\cos\theta)^n]v_\lambda(k_1,k_2;\cos\theta)\,|_{2k_1k_2\cos\theta=0}$$

depends only on k_1^2 and k_2^2, it follows that the terms in Eq. (20) which are odd in $\cos\theta$ are odd in k_1 and k_2 and the terms even in $\cos\theta$ are even in k_1 and k_2. Hence, the terms in the partial-wave expansion of the potential

$$\begin{aligned} v_\lambda(\,|\mathbf{k}_1-\mathbf{k}_2|\,) &= \sum_l v_\lambda^l(k_1,k_2)P_l(\cos\theta) \\ &= 4\pi\sum_l [v_\lambda^l(k_1,k_2)/(2l+1)] \\ &\times \sum_{m=-l}^{l} Y_{l,m}^*(\Omega_1)\,Y_{l,m}(\Omega_2) \\ &\equiv \sum_L v_\lambda^L(k_1,k_2)\,Y_L^*(\Omega_1)\,Y_L(\Omega_2) \end{aligned} \tag{22}$$

must satisfy

$$v_\lambda^L(-k_1,k_2)=(-1)^l v_\lambda^L(k_1,k_2), \tag{23a}$$

$$v_\lambda^L(k_1,-k_2)=(-1)^l v_\lambda^L(k_1,k_2). \tag{23b}$$

The second equality in Eq. (22) follows from the "spherical harmonic addition theorem."[28]

From Eqs. (20) and (23) we see that $t_\lambda^L(k_1,k_2)$ also must satisfy

$$t_\lambda^L(-k_1,k_2)=(-1)^l t_\lambda^L(k_1,k_2), \tag{24a}$$

$$t_\lambda^L(k_1,-k_2)=(-1)^l t_\lambda^L(k_1,k_2). \tag{24b}$$

From Eqs. (23b) and (24a) it follows that the integrand in the second term on the right-hand side (RHS) of Eq. (20) is an even function of k. Thus the limit on the integral may be extended to $-\infty$ and the result evaluated as a simple contour integral. Neglecting possible singularities in the potential v_λ, we obtain

$$\begin{aligned} &\frac{1}{(2\pi)^3}\int_0^\infty dk\,k^2 v_\lambda^L(k_f,k)G(k,E)t_\lambda^L(k,k_i) \\ &= \frac{1}{(2\pi)^3}\frac{1}{2}\int_{-\infty}^{\infty} dk\,k^2 v_\lambda^L(k_f,k)G(k,E)t_\lambda^L(k,k_i) \\ &= -[mi/\hbar^2 8\pi^2]k(E)v_\lambda^L(k_f,k(E))t_\lambda^L(k(E),k_i). \end{aligned} \tag{25}$$

Substituting Eq. (25) into Eq. (20), we obtain

$$\begin{aligned} t_\lambda^L(k_f,k_i) &= v_\lambda^L(k_f,k_i) \\ &- (mi/\hbar^2 8\pi^2)k(E)v_\lambda^L(k_f,k(E))t_\lambda^L(k(E),k_i), \end{aligned} \tag{26}$$

which defines the partial-wave components of the single-site scattering amplitude in terms of the ion-core potential.

The analogous partial-wave decomposition is not so straightforward for Eqs. (3) and (4). The quantity in Eq. (4) corresponding to the ion-core potential is

$$b_\lambda(\mathbf{k}_1,\mathbf{k}_2)=\exp[-W_\lambda(\mathbf{k}_1-\mathbf{k}_2)]t_\lambda(\mathbf{k}_1,\mathbf{k}_2). \tag{27}$$

Although t_λ exhibits the same symmetry properties as v_λ, i.e.,

$$t_\lambda(\mathbf{k}_1,\mathbf{k}_2)=t_\lambda(\,|\mathbf{k}_1-\mathbf{k}_2|\,) \tag{28}$$

unless

$$W_\lambda(\mathbf{k}_1-\mathbf{k}_2)=W_\lambda(\,|\mathbf{k}_1-\mathbf{k}_2|\,) \tag{29}$$

is satisfied, we find

$$b_\lambda(\mathbf{k}_1,\mathbf{k}_2)\neq b_\lambda(\,|\mathbf{k}_1-\mathbf{k}_2|\,). \tag{30}$$

This result, which occurs, e.g., if surface phonons play a role in determining W_λ, complicates the partial-wave decomposition of Eq. (4).

If we use the Debye model[29] for the phonon spectrum of the solid, then Eq. (29) is satisfied. However, even in the case of bulk phonons more realistic models of the spectrum[30] lead to a form of Eq. (10) which does not in general satisfy Eq. (29). Hence in making a partial-wave decomposition we write

$$b_\lambda(\mathbf{k}_1, \mathbf{k}_2) = \sum_{L,L'} b_\lambda^{LL'}(k_1, k_2)\, Y_L^*(\Omega_1)\, Y_{L'}(\Omega_2). \quad (31)$$

We note in passing that $b_\lambda(\mathbf{k}_1, \mathbf{k}_2)$ has the role of the effective single-site scattering amplitude for an electron scattering from an ion core in the solid. Even for a rigid lattice, the use of pseudopotentials[31] may require the general form of Eq. (31) rather than the specialized form of Eq. (16) which resulted from a spherically symmetric ion-core potential. In addition, we do not expect the potentials of the ion cores at the surface of the metal to be spherically symmetric. Hence, we shall take $b_\lambda(\mathbf{k}_1, \mathbf{k}_2)$ as the single-site scattering amplitude and not inquire whether its lack of spherical symmetry comes about from phonon effects or is inherent in the potential of a rigid-ion core.

The partial-wave expansion of Eq. (4) gives

$$\begin{aligned}\sum_{LL'} \tau_\lambda^{LL'}(k_f, k_i)\, Y_L^*(\Omega_f)\, Y_{L'}(\Omega_i) &= \sum_{LL'} b_\lambda^{LL'}(k_f, k_i)\, Y_L^*(\Omega_f)\, Y_{L'}(\Omega_i) \\ &+ \int [(dk)/(2\pi)^3] \sum_{L,L';\ L_1,L_2} b_\lambda^{LL_1}(k_f, k) \\ &\times Y_L^*(\Omega_f)\, Y_{L_1}(\Omega) G^{\mathrm{sp}}(\mathbf{k}, \mathbf{k}_i; E) \\ &\times \tau_\lambda^{L_2L'}(k, k_i)\, Y_{L_2}^*(\Omega)\, Y_{L'}(\Omega_i). \quad (32)\end{aligned}$$

Consequently, we obtain

$$\begin{aligned}\tau_\lambda^{LL'}(k_f, k_i) &= b_\lambda^{LL'}(k_f, k_i) \\ &+ \int [(dk)/(2\pi)^3] \sum_{L_1,L_2} b_\lambda^{LL_1}(k_f, k)\, Y_{L_1}(\Omega) \\ &\times G^{\mathrm{sp}}(\mathbf{k}, \mathbf{k}_i; E) \tau_\lambda^{L_2L'}(k, k_i)\, Y_{L_2}^*(\Omega). \quad (33)\end{aligned}$$

From Eqs. (8) and (13) we can write

$$G^{\mathrm{sp}}(\mathbf{k}, \mathbf{k}_i; E) = G(k, E) \sum_{\mathrm{P}\neq 0} \exp[-i(\mathbf{k}_{||} - \mathbf{k}_{i||})\cdot \mathbf{P}]. \quad (34)$$

We next make use of the angular momentum representation of plane waves,[32]

$$\exp(-i\mathbf{k}\cdot\mathbf{P}) = \sum_{L_3} (4\pi)(-i)^{l_3} Y_{L_3}^*(\Omega)\, Y_{L_3}(\Omega_{\mathrm{P}})\, j_{l_3}(kP), \quad (35)$$

where $j_{l_3}(kP)$ is the spherical Bessel function of order l_3, to write

$$\begin{aligned}G^{\mathrm{sp}}(\mathbf{k}, \mathbf{k}_i, E_i) &= 4\pi G(k, E) \sum_{\mathrm{P}\neq 0} \exp(i\mathbf{k}_i\cdot\mathbf{P}) \\ &\times \sum_{L_3} (-i)^{l_3} Y_{L_3}^*(\Omega)\, Y_{L_3}(\Omega_{\mathrm{P}})\, j_{l_3}(kP). \quad (36)\end{aligned}$$

Substituting Eq. (36) into Eq. (33), we obtain

$$\begin{aligned}\tau_\lambda^{LL'}(k_f, k_i) &= b_\lambda^{LL'}(k_f, k_i) \\ &+ \sum_{L_1,L_2,L_3} \sum_{\mathrm{P}\neq 0} \exp(i\mathbf{k}_i\cdot\mathbf{P})\, Y_{L_3}(\Omega_{\mathrm{P}}) \times \int [(dk)/(2\pi)^3] \\ &\times b_\lambda^{LL_1}(k_f, k)(4\pi)(-i)^{l_3} j_{l_3}(kP) G(k, E) \\ &\times \tau_\lambda^{L_2L'}(k, k_i)\, Y_{L_1}(\Omega)\, Y_{L_2}^*(\Omega)\, Y_{L_3}^*(\Omega). \quad (37)\end{aligned}$$

On the basis of symmetry arguments the integral over $(d\Omega)$ in Eq. (37) is zero unless

$$l_1 + l_2 + l_3 = \text{even number}. \quad (38)$$

In addition, we make use of the symmetry property[33]

$$j_{l_3}(-kP) = (-1)^{l_3} j_{l_3}(kP). \quad (39)$$

The arguments presented in Eqs. (21)–(24) also apply to the $b_\lambda(\mathbf{k}_1, \mathbf{k}_2)$ given by Eq. (5). For appropriate phonon dispersion relations they lead to the relations

$$b_\lambda^{LL_1}(-k_1, k_2) = (-1)^l b_\lambda^{LL_1}(k_1, k_2), \quad (40a)$$

$$b_\lambda^{LL_1}(k_1, -k_2) = (-1)^{l_1} b_\lambda^{LL_1}(k_1, k_2). \quad (40b)$$

From Eqs. (40) and (37) it follows that

$$\tau_\lambda^{L_2L'}(-k_1, k_2) = (-1)^{l_2} \tau_\lambda^{L_2L'}(k_1, k_2), \quad (41a)$$

$$\tau_\lambda^{L_2L'}(k_1, -k_2) = (-1)^{l'} \tau_\lambda^{L_2L'}(k_1, k_2). \quad (41b)$$

Our subsequent analysis is valid only for potentials and phonon dispersion relations such that Eqs. (40) are satisfied. However, this is not a serious restriction.[31] From Eqs. (30)–(41) we see that the integrand in the second term on the RHS of Eq. (37) is an even function of k and so the lower limit can be extended to $-\infty$ and the integral evaluated by contour techniques just as in Eq. (25). Specifically, we find that[34]

$$\begin{aligned}I(L_1, L_2, L_3) &= \int (d\Omega)\, Y_{L_1}(\Omega)\, Y_{L_2}^*(\Omega)\, Y_{L_3}^*(\Omega) \\ &= [(2l_2+1)(2l_3+1)/4\pi(2l_1+1)]^{1/2} C(l_2, l_3, l_1; m_2, m_3, m_1) C(l_2, l_3, l_1; 0, 0, 0), \quad (42)\end{aligned}$$

where

$$\begin{aligned}C(l_2, l_3, l_1; m_2, m_3, m_1) &= \delta_{m_1, m_2+m_3} \{[(2l_1+1)(l_2+l_3-l_1)!/(l_1+l_2+l_3+1)!] \\ &\times (l_1+l_2-l_3)!(l_1+l_3-l_2)!(l_1+m_1)!(l_1-m_1)!(l_2+m_2)!(l_2-m_2)! \times (l_3+m_3)!(l_3-m_3)!\}^{1/2} \\ &\times \sum_\nu [(-1)^\nu/\nu!][(l_2+l_3-l_1-\nu)!(l_2-m_2-\nu)!(l_3+m_3-\nu)!(l_1-l_3+m_2+\nu)!(l_1-l_2-m_3+\nu)!]^{-1}. \quad (43)\end{aligned}$$

As before we shall neglect any possible singular behavior of v_λ in the k plane. This means that only the poles in the electron Green's function enter in the evaluation of Eq. (37) and so we obtain

$$\int_0^\infty dk\, k^2 b_\lambda^{LL_1}(k_f, k) j_{l_3}(kP) G(k, E) \tau_\lambda^{L_2L'}(k, k_i)$$

$$= \frac{1}{2}\int_{-\infty}^{\infty} dk\, k^2 b_\lambda^{LL_1}(k_f, k) j_{l_3}(kP) G(k, E) \tau_\lambda^{L_2L'}(k, k_i)$$

$$= -\frac{m\pi i k(E)}{\hbar^2} b_\lambda^{LL_1}(k_f, k(E)) h_{l_3}^{(1)}(k(E)P) \times \tau_\lambda^{L_2L'}(k(E), k_i). \quad (44)$$

The $h_l^{(1)}(X)$ are spherical Hankel functions (i.e., spherical Bessel functions of the third kind[33]). In Sec. III we investigate the number of partial waves necessary for a reasonable model calculation and give explicit expressions for the $h_l^{(1)}$. Using Eqs. (42) and (44), we can rewrite Eq. (37) as

$$\tau_\lambda^{LL'}(k_f, k_i) = b_\lambda^{LL'}(k_f, k_i) + \sum_{L_1,L_2} b_\lambda^{LL_1}(k_f, k(E)) \times \Big(\sum_{\mathbf{P}\neq 0} \exp(i\mathbf{k}_i\cdot\mathbf{P}) \sum_{L_3} \frac{(4\pi)(-i)^{l_3}}{(2\pi)^3} \frac{-m\pi i k(E)}{\hbar^2} \times h_{l_3}^{(1)}(k(E)P) Y_{L_3}(\Omega_\mathbf{P}) I(L_1, L_2, L_3) \Big) \tau_\lambda^{L_3L'}(k(E), k_i). \quad (45)$$

Equation (45) can be written in a compact notation by defining[34]

$$G_{L_1L_2}^{\mathrm{sp}}(\mathbf{k}_i) = \sum_{\mathbf{P}\neq 0} \exp(i\mathbf{k}_i\cdot\mathbf{P}) \sum_{L_3} \frac{(-i)^{l_3}}{2\pi^2} \frac{-m\pi i k(E)}{\hbar^2} \times h_{l_3}^{(1)}(k(E)P) Y_{L_3}(\Omega_\mathbf{P}) I(L_1, L_2, L_3) = \sum_{\mathbf{P}\neq 0} \exp(i\mathbf{k}_i\cdot\mathbf{P}) G_{L_1L_2}^{\mathrm{sp}}(\mathbf{P}). \quad (46)$$

In terms of $G_{L_1L_2}^{\mathrm{sp}}(\mathbf{k}_i)$, Eq. (45) becomes

$$\tau_\lambda^{LL'}(k_f, k_i) = b_\lambda^{LL'}(k_f, k_i) + \sum_{L_1,L_2} b_\lambda^{LL_1}(k_f, k(E)) G_{L_1L_2}^{\mathrm{sp}}(\mathbf{k}_i) \tau_\lambda^{L_2L'}(k(E), k_i). \quad (47)$$

The partial-wave decomposition of Eq. (3) follows in a completely analogous manner. Writing

$$T_\lambda(\mathbf{k}_f, \mathbf{k}_i) = \sum_{LL'} T_\lambda^{LL'}(k_f, k_i) Y_L^*(\Omega_f) Y_{L'}(\Omega_i), \quad (48)$$

we find

$$T_\lambda^{LL'}(k_f, k_i) = \tau_\lambda^{LL'}(k_f, k_i) + \sum_{\lambda_1\neq\lambda} \sum_{L_1,L_2} \tau_\lambda^{LL_1}(k_f, k(E)) \times G_{L_1L_2}^{\lambda\lambda_1}(\mathbf{k}_i) T_{\lambda_1}^{L_2L'}(k(E), k_i), \quad (49)$$

where

$$G_{L_1L_2}^{\lambda\lambda_1}(\mathbf{k}_i) = \sum_{\mathbf{P}} \exp\{i\mathbf{k}_i\cdot[\mathbf{P}+\mathbf{a}(\lambda_1-\lambda)+(d_{\lambda_1}-d_\lambda)\hat{z}]\} \times G_{L_1L_2}^{\lambda\lambda_1}(\mathbf{P}) \quad (50)$$

and[16]

$$G_{L_1L_2}^{\lambda\lambda_1}(\mathbf{P}) = \sum_{L_3} \frac{(-i)^{l_3}}{2\pi^2} \frac{-m\pi i k(E)}{\hbar^2} \times h_{l_3}^{(1)}(k(E)\,|\,\mathbf{P}+\mathbf{a}(\lambda_1-\lambda)+(d_{\lambda_1}-d_\lambda)\hat{z}\,|) \times Y_{L_3}(\Omega_{\mathbf{P}+\mathbf{a}(\lambda_1-\lambda)+(d_{\lambda_1}-d_\lambda)\hat{z}}) I(L_1, L_2, L_3). \quad (51)$$

In deriving Eqs. (26), (47), and (49) we have made use of the properties of the vertex functions for general values of the momenta. However, now that we have derived these equations we note that we are considering the elastic scattering cross section. Therefore we require the t amplitudes only for values of k_i and k_f such that

$$k_i = k_f = k(E), \quad (52)$$

i.e., we say that the t amplitudes are evaluated "on the energy shell." Thus, on the energy shell we have for Eqs. (26), (47), and (49)

$$t_\lambda^L(k(E)) = v_\lambda^L(k(E)) - \frac{mik(E)}{\hbar^2 8\pi^2} v_\lambda^L(k(E)) t_\lambda^L(k(E)), \quad (53)$$

$$\tau_\lambda^{LL'}(k(E)) = b_\lambda^{LL'}(k(E)) + \sum_{L_1,L_2} b_\lambda^{LL_1}(k(E)) G_{L_1L_2}^{\mathrm{sp}}(\mathbf{k}_i) \tau_\lambda^{L_2L'}(k(E)), \quad (54)$$

$$T_\lambda^{LL'}(k(E)) = \tau_\lambda^{LL'}(k(E)) + \sum_{L_1,L_2} \sum_{\lambda_1\neq\lambda} \tau_\lambda^{LL_1}(k(E)) G_{L_1L_2}^{\lambda\lambda_1}(\mathbf{k}_i) T_{\lambda_1}^{L_2L'}(k(E)), \quad (55)$$

where the energy-shell values of $b(\mathbf{k}_1, \mathbf{k}_2)$ are related to the energy-shell values of $t(\mathbf{k}_1, \mathbf{k}_2)$ through Eq. (5). Thus the solution to Eqs. (53)–(55) requires the evaluation of $W_\lambda(\mathbf{k}_1-\mathbf{k}_2)$, which in turn requires a model of the phonon spectrum of the solid. We defer further discussion of this point until Sec. III, where we make use of a specific model for the phonon spectrum.

Equations (48) and (53)–(55) completely specify the momentum space representation of the scattering amplitude as a set of coupled algebraic equations. The scattering amplitude through Eqs. (1) and (2) then determines the elastic scattering cross section. Our equations represent the appropriate generalization of Beeby's[27] analysis of the muffin-tin model which is needed to describe the influence of lattice vibrations on the elastic scattering cross section. An interesting feature of these equations is that they are no more complicated than Beeby's. However, we have avoided both the muffin-tin restriction that the potentials be nonoverlapping and the requirement that the potentials be spherically symmetric. Again we point out that $b_\lambda(\mathbf{k}_1, \mathbf{k}_2)$ has the role of an effective single-site scattering amplitude and whether its asymmetry and extended nature come from phonon effects or from the nature of the potential $v_n(\mathbf{r}-\mathbf{R}_n)$ is irrelevant in our analysis.

In closing this section we note that if the effective site potential were spherically symmetric, we would

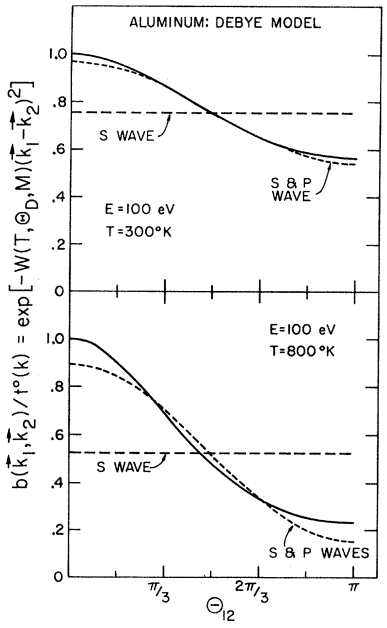

FIG. 1. Plot of effective site scattering amplitude divided by the rigid-ion scattering amplitude versus scattering angle. The parameters used in making the plot are for bulk aluminum ($M=27$ amu, $\Theta_D=426$°K). The horizontal dashed line shows the s-wave approximation to the scattering vertex and the dotted line shows the approximation of using both s and p waves. The electron self-energy has been taken to be zero.

have

$$b_\lambda^{L_1L_2}(k(E))=b_\lambda^{L_1}(k(E))\delta_{L_1,L_2}, \tag{56}$$

and Eq. (54) would have the simplified form

$$\tau_\lambda^{LL'}(k(E))=b_\lambda^{L}(k(E))\delta_{L,L'} + \sum_{L_2} b_\lambda^{L}(k(E))G_{LL_2}^{\rm sp}(\mathbf{k}_i)\tau_\lambda^{L_2L'}(k(E)). \tag{57}$$

In the case that we consider only the $L=L'=0$ components of both $T^{LL'}$ and $G_{LL'}$, we recover the isotropic-scatterer inelastic collision model.[3–5]

III. MODEL FOR NUMERICAL CALCULATIONS

We shall illustrate the effect of temperature upon the elastic scattering cross section through a very simple model—namely, use of s-wave scattering from a rigid-ion core, use of the Debye model[29] to characterize the phonon spectrum of the solid, and inclusion of lattice expansion in an empirical manner.[35] We also assume that only the surface layer of atoms is different from the layers of atoms making up the "bulk" of the solid. We do not specify the potential in Eq. (26) but instead will treat the phase shift as a parameter in our calculation.[1,3–6] The amplitude for scattering from a rigid-ion core is written as

$$t_S^0(k(E))=[\pi i\hbar^2/mk(E)](e^{2i\delta_S}-1) \tag{58}$$

for an ion core at the surface and as

$$t_B^0(k(E))=[\pi i\hbar^2/mk(E)](e^{2i\delta_B}-1) \tag{59}$$

for an ion core in the "bulk." The effective single-site scattering amplitude is obtained from Eq. (5),

$$b_\lambda(\mathbf{k}_1,\mathbf{k}_2)=t_\lambda^0(k(E))\exp[-W_\lambda(\mathbf{k}_1-\mathbf{k}_2)]. \tag{60}$$

The Debye model of the phonon spectrum gives the expression for W_λ

$$W_\lambda(\mathbf{k}_1-\mathbf{k}_2)=\frac{3\hbar^2(\mathbf{k}_1-\mathbf{k}_2)^2}{2Mk_B\Theta_D^\lambda} \times\left[\frac{1}{4}+\left(\frac{T}{\Theta_D^\lambda}\right)^2\int_0^{\Theta_D^\lambda/T}dx\,\frac{x}{e^x-1}\right] \equiv W(T,\Theta_D^\lambda,M)(\mathbf{k}_1-\mathbf{k}_2)^2. \tag{61}$$

In Eq. (61) Θ_D^λ is the Debye temperature characterizing the vibration of an atom in the λth layer and T is the temperature of the system. The effective single-site scattering amplitude given in Eq. (60) no longer describes only s-wave scattering since the $\exp[-W_\lambda(\mathbf{k}_1-\mathbf{k}_2)]$ factor introduces higher partial waves. To make this point more explicit let us take our solid to be aluminum. In Fig. 1 we see a plot of $b_\lambda(\mathbf{k}_1,\mathbf{k}_2)/t_\lambda^0(k(E))$ versus scattering angle for parameters corresponding to bulk aluminum. In this figure we also show both the s- and the $(s+p)$-wave approximations to the scattering vertex. Clearly a reasonable description of the scattering vertex requires the use of more than simply s waves. As we are examining only a simple model of the solid to illustrate the effect of lattice vibrations, in the interest of computational simplicity we restrict our analysis to only s and p waves.

In Sec. II we generated a set of matrix equations for the scattering amplitude $T_\lambda(\mathbf{k}_f,\mathbf{k}_i;E)$. The full solution of these equations would correspond to the "matrix inversion" procedure of Tucker and Duke.[5] However, it seems most feasible to proceed in the present case as in the rigid-lattice case by first examining the consequences of the double-diffraction approximation and then turning to the matrix inversion calculation.[3–5] This procedure has the advantage that in the double-diffraction approximation we can isolate explicitly the dynamical origin of peaks in the intensity profile and, consequently, distinguish between intralayer multiple-scattering peaks, primary Bragg peaks, and secondary Bragg peaks. In addition, for small phase shifts the results of second-order perturbation theory are in reasonable agreement with those of the more accurate "matrix inversion" procedure.[5] As aluminum is a weak scattering material, we might expect the double-diffraction analysis to be adequate for it.

Following Duke, Anderson, and Tucker,[4] we have through second order in the planar scattering amplitudes,

$$T_\lambda(\mathbf{k}_f,\mathbf{k}_i)=\tau_\lambda(\mathbf{k}_f,\mathbf{k}_i)+\int[(dk)/(2\pi)^3] \times\sum_{\lambda_1\neq\lambda}\tau_\lambda(\mathbf{k}_f,\mathbf{k})G^{\lambda\lambda_1}(\mathbf{k},\mathbf{k}_i,E)\tau_{\lambda_1}(\mathbf{k},\mathbf{k}_i). \tag{62}$$

Making a partial-wave decomposition of T_λ and τ_λ in Eq. (62) and using the explicit form of $G^{\lambda\lambda_1}$, we obtain

$$T_\lambda^{LL'}(k_f, k_i)=\tau_\lambda^{LL'}(k_f, k_i)+\int[(dk)/(2\pi)^3]\sum_{\lambda_1\neq\lambda}\sum_{L_1,L_2}\tau_\lambda^{LL_1}(k_f, k)\,Y_{L_1}(\Omega)\times\sum_{\mathrm{P}}\exp\{-i[\mathbf{k}_{||}-\mathbf{k}_{i||}]\cdot[\mathbf{P}+\mathbf{a}(\lambda_1-\lambda)]-i(k_\perp-k_{i\perp})(d_{\lambda_1}-d_\lambda)\}\times G(k, E)\,Y_{L_2}^*(\Omega)\tau_{\lambda_1}^{L_2L}(k, k_i). \quad (63)$$

In Eq. (63) we first perform the sum over $\mathbf{P}$ to obtain

$$\sum_{\mathrm{P}}\exp[-i(\mathbf{k}_{||}-\mathbf{k}_{i||})\cdot\mathbf{P}]=N_{||}\sum_{\mathbf{g}'}\delta(\mathbf{k}_{||}-\mathbf{k}_{i||}-\mathbf{g}'). \quad (64)$$

We then use the δ function in Eq. (64) to perform the part of the integral in Eq. (53) over $\mathbf{k}_{||}$. In doing this integral we consider the $Y_L(\Omega)$ to be functions of $\mathbf{k}$; i.e., we take

$$Y_L(\Omega)\equiv Y_L(\mathbf{k}_{||}, k_\perp). \quad (65)$$

We thus obtain

$$T_\lambda^{LL'}(k_f, k_i)=\tau_\lambda^{LL'}(k_f, k_i)-\left(\frac{2m}{\hbar^2}\right)\frac{N_{||}}{(2\pi)^2}\int\frac{dk_\perp}{2\pi}\sum_{\mathbf{g}'}\sum_{\lambda_1\neq\lambda}\sum_{L_1,L_2}\times\frac{\tau_\lambda^{LL_1}(k_f, |\mathbf{k}_{i||}+\mathbf{g}'+k_\perp\hat{z}|)\exp[-i\mathbf{g}'\cdot\mathbf{a}(\lambda_1-\lambda)-i(k_\perp-k_{i\perp})(d_{\lambda_1}-d_\lambda)]Y_{L_1}(\mathbf{k}_{i||}+\mathbf{g}', k_\perp)}{k_\perp^2-k_\perp^2(\mathbf{g}', E)}\times Y_{L_2}^*(\mathbf{k}_{i||}+\mathbf{g}', k_\perp)\tau_\lambda^{L_2L'}(|\mathbf{k}_{i||}+\mathbf{g}'+k_\perp\hat{z}|, k_i), \quad (66)$$

where

$$k_\perp^2(\mathbf{g}', E)=(2m/\hbar^2)[E-\Sigma(E)]-(\mathbf{k}_{i||}+\mathbf{g}')^2. \quad (67)$$

In Eq. (66) the integral over dk can be done by way of a contour integration. For $(d_{\lambda_1}-d_\lambda)<0$ we close the contour in the upper half-plane and for $(d_{\lambda_1}-d_\lambda)>0$ we close the contour in the lower half-plane. Since

$$|\mathbf{k}_{i||}+\mathbf{g}'\pm k_\perp(\mathbf{g}', E)\hat{z}|=k(E), \quad (68)$$

we can write our result as

$$T_\lambda^{LL'}(k_f, k_i)=\tau_\lambda^{LL'}(k_f, k_i)-(mi/\hbar^2)[N_{||}/(2\pi)^2]\sum_{g'}\sum_{L_1,L_2}[k_\perp(\mathbf{g}', E)]^{-1}\times\{\sum_{\lambda_1>\lambda}\exp[-i\mathbf{g}'\cdot\mathbf{a}(\lambda_1-\lambda)+i(k_\perp(\mathbf{g}, E_i)+k_{i\perp})(d_{\lambda_1}-d_\lambda)]\tau_\lambda^{LL_1}(k_f, k(E))\times Y_{L_1}(\mathbf{k}_{i||}+\mathbf{g}', -k_\perp(\mathbf{g}', E))Y_{L_2}^*(\mathbf{k}_{i||}+\mathbf{g}', -k_\perp(\mathbf{g}', E))\tau_{\lambda_1}^{L_2L'}(k(E), k_i)+\sum_{\lambda_1<\lambda}\exp[-i\mathbf{g}'\cdot\mathbf{a}(\lambda_1-\lambda)-i(k_\perp(\mathbf{g}', E_i)-k_{i\perp})(d_{\lambda_1}-d_\lambda)]\tau_\lambda^{LL_1}(k_f, k(E))\times Y_{L_1}(\mathbf{k}_{i||}+\mathbf{g}', k_\perp(\mathbf{g}', E))Y_{L_2}^*(\mathbf{k}_{i||}+\mathbf{g}', k_\perp(\mathbf{g}', E))\tau_{\lambda_1}^{L_2L'}(k(E), k_i)\}. \quad (69)$$

Substituting Eq. (69) into Eq. (2), we explicitly perform the sums over λ and λ_1. Assuming that only the surface layer scatters differently from the "bulk" layers and that successive layers are spaced a distance "d" apart, the final result can be written as

$$I(\mathbf{k}_f, \mathbf{k}_i; E)=N_{||}\sum_{\mathbf{g}}\sum_{L,L'}\delta(\mathbf{k}_{f||}-\mathbf{k}_{i||}-\mathbf{g})\,Y_L^*(\mathbf{k}_{i||}+\mathbf{g}, -k_\perp(\mathbf{g}, E))\times Y_{L'}(\mathbf{k}_{i||}, k_\perp(0, E))\left\{\left(\tau_S^{LL'}(k(E))+\frac{R(0, \mathbf{g}; E)\exp(-i\mathbf{a}\cdot\mathbf{g})\tau_B^{LL'}(k(E))}{1-R(0, \mathbf{g}; E)\exp(-i\mathbf{a}\cdot\mathbf{g})}\right)-\frac{mi}{\hbar^2}\frac{N_{||}}{(2\pi)^2}\sum_{\mathbf{g}'}\sum_{L_1,L_2}[k_\perp(\mathbf{g}', E)]^{-1}\left[\frac{R(0, \mathbf{g}', E)\exp(-i\mathbf{a}\cdot\mathbf{g}')}{1-R(0, \mathbf{g}', E)\exp(-i\mathbf{a}\cdot\mathbf{g}')}\right.\times\left(\tau_S^{LL_1}(k(E))\tau_B^{L_2L'}(k(E))+\frac{R(0, \mathbf{g}; E)\exp(-i\mathbf{a}\cdot\mathbf{g})}{1-R(0, \mathbf{g}; E)\exp(-i\mathbf{a}\cdot\mathbf{g})}\tau_B^{LL_1}(k(E))\tau_B^{L_2L'}(k(E))\right)\times Y_{L_1}(\mathbf{k}_{i||}+\mathbf{g}', -k_\perp(\mathbf{g}', E))Y_{L_2}^*(\mathbf{k}_{i||}+\mathbf{g}'-k_\perp(\mathbf{g}', E))+\frac{R(\mathbf{g}, \mathbf{g}', E)\exp[-i\mathbf{a}\cdot(\mathbf{g}-\mathbf{g}')]}{1-R(\mathbf{g}, \mathbf{g}', E)\exp[-i\mathbf{a}\cdot(\mathbf{g}-\mathbf{g}')]}\times\left(\tau_B^{LL_1}(k(E))\tau_S^{L_2L'}(k(E))+\frac{R(0, \mathbf{g}; E)\exp(-i\mathbf{a}\cdot\mathbf{g})}{1-R(0, \mathbf{g}; E)\exp(-i\mathbf{a}\cdot\mathbf{g})}\tau_B^{LL_1}(k(E))\tau_B^{L_2L'}(k(E))\right)\times Y_{L_1}(\mathbf{k}_{i||}+\mathbf{g}', k_\perp(\mathbf{g}', E))Y_{L_2}^*(\mathbf{k}_{i||}+\mathbf{g}', k_\perp(\mathbf{g}', E))\left.\right]\right\}=N_{||}\sum_{\mathbf{g}}\delta(\mathbf{k}_{f||}-\mathbf{k}_{i||}-\mathbf{g})A_{\mathbf{g}}. \quad (70)$$

In Eq. (70) the symbol R is defined by

$$R(\mathbf{g}, \mathbf{g}', E) \equiv \exp(id[k_\perp(\mathbf{g}, E) + k_\perp(\mathbf{g}', E)]), \tag{71}$$

$\tau_S^{LL'}(k(E))$ denotes the scattering amplitude for the surface layer, and $\tau_B^{LL'}(k(E))$ denotes the scattering amplitude for a bulk layer.

Equations (1), (57), and (70) determine the elastic scattering cross section in terms of the spherically symmetric single-site scattering amplitudes of our model. Specifically we find for the partial-wave components of the single-site scattering amplitude

$$b_\lambda^L(k(E)) = t_\lambda^0(k(E)) e^{-2wk^2(E)} (4\pi) S_0(k(E)), \qquad L = (0, 0) \tag{72a}$$

and

$$b_\lambda^L(k(E)) = t_\lambda^0(k(E)) e^{-2wk^2(E)} \tfrac{4}{3}\pi S_1(k(E)), \qquad L = (1, 1), (1, 0), (1, -1) \tag{72b}$$

where

$$w = W(T, \Theta_D^\lambda, M), \tag{73}$$

$$S_0(k(E)) = \sinh 2wk^2(E)/2wk^2(E) \tag{74}$$

and

$$S_1(k(E)) = [3/2wk^2(E)]\{\cosh 2wk^2(E) - [\sinh 2wk^2(E)/2wk^2(E)]\}. \tag{75}$$

In matrix notation, Eq. (57) becomes

$$\overleftrightarrow{\tau}_\lambda(K(E)) = \overleftrightarrow{b}_\lambda(K(E)) + \overleftrightarrow{b}_\lambda(K(E)) \overleftrightarrow{G}^{sp}(\mathbf{k}_i) \overleftrightarrow{\tau}_\lambda(K(E)). \tag{76}$$

Formally, Eq. (76) easily can be inverted to give

$$\overleftrightarrow{\tau}_\lambda(K(E)) = [\overleftrightarrow{I} - \overleftrightarrow{b}_\lambda(k(E)) \overleftrightarrow{G}^{sp}(\mathbf{k}_i)]^{-1} \overleftrightarrow{b}_\lambda(k(E)). \tag{77}$$

The matrices in Eqs. (76) and (77) are 4×4 in dimension with $\overleftrightarrow{I}$ being the identity matrix. As the components of $\overleftrightarrow{b}_\lambda(k(E))$ are specified by Eq. (72), all that remains is to determine $\overleftrightarrow{G}^{sp}(\mathbf{k}_i)$ in order to specify the second-order perturbation-theory solution. Defining

$$\overleftrightarrow{G}^{sp}(\mathbf{k}_i) = \frac{2m}{\hbar^2} \frac{k(E)}{16\pi^2} \sum_{P \neq 0} \overleftrightarrow{G}^{sp}(\mathbf{P}) \exp[i\mathbf{k}_i \cdot \mathbf{P}], \tag{78}$$

we find from Eq. (46)

$$\overleftrightarrow{G}^{sp}(\mathbf{P}) = \begin{bmatrix} [-ih_0^{(1)}(X)] & [-e^{i\phi}h_1^{(1)}(X)\sqrt{\tfrac{3}{2}}] & 0 & [e^{-i\phi}h_1^{(1)}(X)\sqrt{\tfrac{3}{2}}] \\ [-e^{-i\phi}h_1^{(1)}(X)\sqrt{\tfrac{3}{2}}] & [-ih_0^{(1)}(X) + \tfrac{1}{2}ih_2^{(1)}(X)] & 0 & [-\tfrac{3}{2}ie^{-2i\phi}h_2^{(1)}(X)] \\ 0 & 0 & [-ih_0^{(1)}(X) - ih_2^{(1)}(X)] & 0 \\ [e^{i\phi}h_1^{(1)}(X)\sqrt{\tfrac{3}{2}}] & [-\tfrac{3}{2}ie^{2i\phi}h_2^{(1)}(X)] & 0 & [-ih_0^{(1)}(X) + \tfrac{1}{2}ih_2^{(1)}(X)] \end{bmatrix}, \tag{79}$$

where

$$X \equiv k(E)P, \tag{80a}$$

$$h_0^{(1)}(X) = -ie^{iX}/X, \tag{80b}$$

$$h_1^{(1)}(X) = e^{iX}[-i/X^2 - 1/X], \tag{80c}$$

$$h_2^{(1)}(X) = e^{iX}[-3i/X^3 - 3/X^2 + i/X], \tag{80d}$$

and $\phi = \phi(\mathbf{P})$ is the azimuthal angle corresponding to the vector $\mathbf{P}$.

Finally to determine $k(E)$ we need to specify the electron self-energy. We take[1,3–5]

$$\Sigma(E) = -V_0 - i\Gamma(E), \tag{81}$$

where V_0 is the inner potential which should be approximately equal to the work function plus the Fermi energy for a "free-electron" metal and

$$\Gamma(E) = (\hbar^2/m\lambda_{ee})(2mE/\hbar^2 + 2mV_0/\hbar^2)^{1/2}. \tag{82}$$

In Eq. (82) λ_{ee} is twice the electron inelastic-collision mean free path and is treated as a parameter in the calculation.

IV. NUMERICAL RESULTS

In this section we discuss the results of our calculation of the elastic scattering cross section. We have assumed only s-wave scattering from a rigid-ion core and have used the Debye model for the phonon spectrum of the solid. The parameters of the calculation have been chosen to correspond to the (00) beam normally incident upon Al(100).

A change in temperature affects the elastic scattering cross section in two ways: (a) It causes a change in the lattice constant which can produce a significant shift in the position of the peaks and (b) it causes a change in the vibrational amplitude of the ion cores which can produce a significant change in peak height. In previous works,[22–26] experimental data on the temperature dependence of the elastic LEED energy profile have been analyzed using the Born approximation to describe the electron-lattice interaction. Although these analyses are not identical (because of their varying assumptions about the inelastic-collision penetration depth of the incident electrons into the lattice), they share one common feature: the use of Eq. (10) to extract from the data semiquantitative information about the mean atomic displacements $\langle u_\lambda^2\rangle_T$, in the surface layers. A major result of the analyses is the observation that $\langle u_{\lambda\perp}^2\rangle_T$ appears to depend explicitly on the energy of the incident electron beam. In particular, $\langle u_{\lambda\perp}^2\rangle_T$ decreases as the beam energy increases from a "surface" value at low beam energies ($E\sim 20$ eV) to the "bulk" value at higher beam energies ($E>200$ eV). An attempt to describe this phenomenon quantitatively using the kinematical approach has been given by Jones, McKinney, and Webb.[24] They utilized simple models for $\langle u_{\lambda\perp}^2\rangle_T$ as a function of λ and an empirically determined dependence of the inelastic-collision damping on the energy of the incident beam. Any such model in which the inelastic-collision damping is taken to decrease with increasing energy describes the qualitative features of the data. No one, including Jones *et al.*,[24] has provided a semiquantitative description of the details of the data. Our approach in this section is to investigate the sensitivity of the predictions of our double-diffraction model to the values of the parameters used in the calculation. In addition to being based on a dynamical model, our analysis differs from previous ones[22–26] also because we consider the influence on its predictions of the different elastic scattering properties of surface and bulk ion cores.[36,37] In fact, one of our major conclusions is the observation that although an effective Debye temperature can be assigned to each peak in the energy profile, in general this effective Debye temperature is not simply related to the rms vibrational amplitudes of the ion cores. The model predictions do not seem to permit a well-defined distinction to be drawn between the consequences of the vibronic inequivalence of the surface and bulk layers and those of their electronic inequivalence.

We first investigate the effect of a change only in lattice constant. This is shown in Fig. 2 for a rigid lattice of ion cores. Note that a change in the lattice constant causes a significant shift in peak position but negligible change in peak height. Although it is a trivial

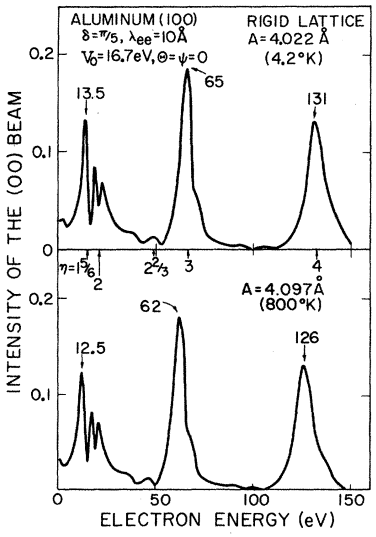

FIG. 2. Elastic energy profiles for the parameters shown in the figure. The calculation was performed for a rigid lattice taking both the surface and the bulk ion cores to exhibit a phase shift of $\frac{1}{5}\pi$. The positions of several peaks are given in eV.

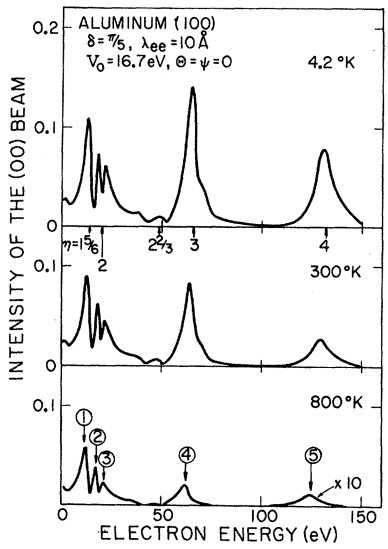

FIG. 3. Elastic energy profiles for a vibrating lattice. The surface and bulk ion cores were assumed to be both electronically and vibronically equivalent. The scattering phase shift of an ion core was taken as $\frac{1}{5}\pi$ and the Debye temperature characterizing the vibrational motion was taken as 426°K. The other parameters of the calculation are indicated in the figure. The circled numbers label the various peaks for reference in Fig. 4.

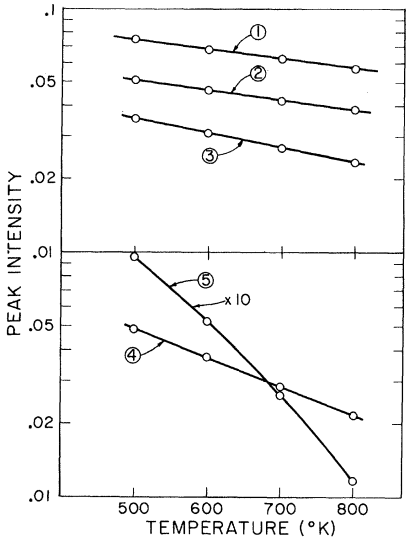

FIG. 4. Plot of the logarithm of peak intensity versus temperature for the peaks shown in Fig. 3.

effect, this shift in peak position clearly must be taken into account in any experimental measurement of the effect of temperature upon peak height.[24,38]

In Fig. 3 we illustrate the influence of both the change in the lattice constant and the change in the vibrational amplitude of the ion cores with a change in the temperature of the system. Note that not only the over-all height of the energy profile changes with temperature, but also the relative heights of the peaks within a given profile can change. From the size of the effect it is apparent that the temperature of the sample is an important parameter in a quantitative theory of LEED.

As described earlier, a common way of analyzing experimental energy profiles is to try to identify the Bragg peaks and then to analyze their temperature dependence using the Born approximation (kinematical approach) to describe the scattering.[22–26] In this approximation the intensity of a Bragg peak is expected to behave like

$$I=I_0\exp[-2W(T,\Theta_D,M)(\mathbf{k}_f-\mathbf{k}_i)^2]. \quad (83)$$

From the form of $W(T,\Theta_D,M)$ given in Eq. (61) we see that for $T\gg\Theta_D$ we expect

$$W(T,\Theta_D,M)\rightarrow 3\hbar^2T/2Mk_B\Theta_D^2. \quad (84)$$

Hence, a plot of $\log I$ versus T (for $T\gg\Theta_D$) should yield a straight line from the slope of which one can obtain an effective Θ_D. One possible problem even in the double-diffraction approximation is that of distinguishing the Bragg peaks from the intralayer multiple-scattering peaks.[4,5] Therefore, it is of interest to determine whether the above procedure can serve as a diagnostic for "primary Bragg peaks." In Fig. 4 we perform such an analysis for all of the peaks shown in Fig. 3. In this particular case peaks 4 and 5 are primary Bragg peaks; peak 1 is an intralayer multiple-scattering peak, and peaks 2 and 3 are the split $n=2$ primary Bragg peak. Except for peak 5 both Bragg peaks and multiple-scattering peaks gave good straight lines on a semilogarithmic plot of $\log I$ versus temperature. The curvature of the line for peak 5 is due to the failure of the expansion of the Debye-Waller factor using only s and p waves. The breakdown of the expansion happens first for peak 5 because of its higher energy. Using the input inner potential of 16.7 eV, we find the following effective Debye temperatures for the first four peaks:

$$\Theta_D(1)=429°\text{K}, \quad (85a)$$

$$\Theta_D(2)=456°\text{K}, \quad (85b)$$

$$\Theta_D(3)=395°\text{K}, \quad (85c)$$

$$\Theta_D(4)=407°\text{K}. \quad (85d)$$

There is about a 5% scatter in these values about the known input $\Theta_D=426°$K. Such scatter in effective Debye temperatures from a mean value is apparent in the experimental work of Refs. 24–26.

The parameters used for the plot in Fig. 3 represent the special case of equivalent surface and bulk ion cores. In a real material we expect the surface ions to have a larger vibrational amplitude than the bulk

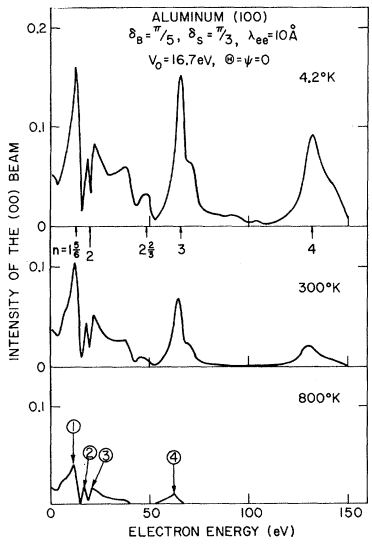

FIG. 5. Elastic energy profiles for a vibrating lattice. The surface and bulk ion cores were assumed to be inequivalent electronically and vibronically. The effective Debye temperature for the surface layer is $\Theta_D{}^S=300°$K and for the bulk layers is $\Theta_D{}^B=426°$K. The other parameters of the calculation are indicated in the figure. Because of the complete breakdown of the Debye-Waller factor expansion for the surface layer at high energies and temperature, we do not show the $n=4$ primary Bragg peak in the bottom panel. The circled numbers label the various peaks for reference in Fig. 6.

ions[24–26] and also we expect that the surface ions might be screened less effectively by the conduction electrons and hence interact differently with the electron beam than the bulk ions do.[36,37] In Fig. 5 we show an energy profile for a case in which the surface ion cores are inequivalent both vibronically and electronically to the bulk ion cores. The additional multiple-scattering structure due to the larger surface layer phase shift is apparent when we compare Figs. 3 and 5. The choice of Debye temperatures for the bulk and surface layers gives a surface ion core about twice the mean-square vibrational amplitude of the bulk ion cores at high temperatures.

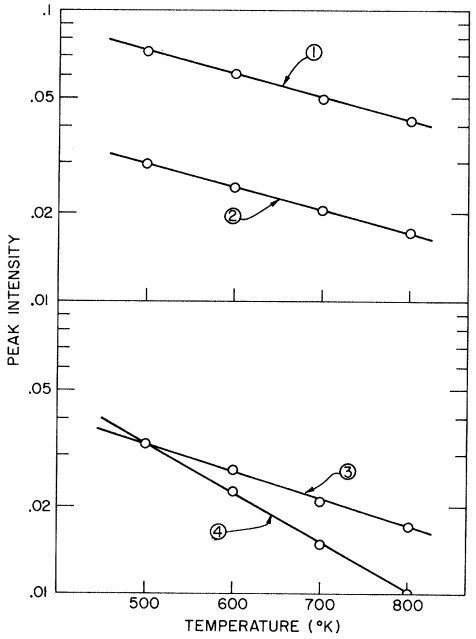

FIG. 6. Plot of the logarithm of peak height versus temperature for the peaks shown in Fig. 5.

Figure 6 shows the results of a Born-approximation analysis of the temperature dependence of the peaks shown in Fig. 5. In this case also good straight lines are obtained both for the "Bragg" peaks and the multiple-scattering peaks. We obtain the following effective Debye temperatures for the first four peaks:

$$\Theta_D(1)=299°\text{K}, \tag{86a}$$

$$\Theta_D(2)=323°\text{K}, \tag{86b}$$

$$\Theta_D(3)=311°\text{K}, \tag{86c}$$

$$\Theta_D(4)=336°\text{K}. \tag{86d}$$

Again we notice about a 5% scatter in the values obtained. We also note that although the effective Debye temperatures are greatly influenced by the surface layer, for the Bragg peaks the effective Debye temperatures lie between the surface and the bulk values as might be expected.

TABLE I. Influence of surface-layer scattering on effective Debye temperature for vibronically equivalent surface and bulk ion-core potentials. Parameters of the calculation: $\lambda_{ee}=10$ Å, $\Theta_D{}^B=\Theta_D{}^S=426°\text{K}$, $\delta_B=\frac{1}{5}\pi$.

Peak	Energy[a] (eV)	$\delta_S=\frac{1}{5}\pi$ (°K)	$\delta_S=\frac{1}{4}\pi$ (°K)	$\delta_S=\frac{1}{3}\pi$ (°K)
1	12.5	429	428	427
2	18	456	437	432
3	21.5	395	417	402
4 (Bragg)	63	407	409	403

[a] Peak position used in determining effective Debye temperatures (position at 600°K).

Having established that both "Bragg" peaks and multiple-scattering peaks can be characterized by an effective Debye temperature,[39] we proceed to investigate the dependence of the effective Debye temperature on the parameters of the model. In Table I we show the effect of varying the scattering power of the surface ions relative to that of the bulk ions for the case of all ions being vibronically equivalent. Although there is some shift in the effective Debye temperatures, all values remain within about ±5% of the input Debye temperature of 426°K.

In Table II we show the effect of varying the vibrational amplitude of the surface ions relative to the vibrational amplitude of the bulk ions for the case of all ions being electronically equivalent. The vibrational amplitude of the surface layer has a large effect on the values of the effective Debye temperatures. In all cases the effective Debye temperature decreases when the surface layer Debye temperature is decreased. However, we note that the effective Debye temperature is always between the surface and the bulk values. This is because the electrons penetrate the solid to some degree and do not simply scatter from the surface layer.

In Table III we show the effect of varying the scattering power of the surface ions relative to that

TABLE II. Influence of surface-layer vibration on effective Debye temperature for electronically equivalent surface and bulk ion-core potentials. Parameters of the calculation: $\lambda_{ee}=10$ Å, $\Theta_D{}^B=426°\text{K}$, $\delta_B=\delta_S=\frac{1}{5}\pi$.

Peak	Energy[a] (eV)	$\Theta_D{}^S=426°\text{K}$ (°K)	$\Theta_D{}^S=360°\text{K}$ (°K)	$\Theta_D{}^S=300°\text{K}$ (°K)
1	12.5	429	389	335
2	18	456	377	341
3	21.5	395	360	308
4 (Bragg)	63	407	386	359

[a] Peak position used in determining effective Debye temperatures (position at 600°K).

TABLE III. Influence of surface-layer scattering on effective Debye temperature for a vibronically inequivalent surface layer of ion-core potentials. Parameters of the calculation: $\lambda_{ee}=10$ Å, $\Theta_D{}^B=426°\text{K}$, $\Theta_D{}^S=300°\text{K}$, $\delta_B=\frac{1}{5}\pi$.

Peak	Energy[a] (eV)	$\delta_S=\frac{1}{5}\pi$ (°K)	$\delta_S=\frac{1}{4}\pi$ (°K)	$\delta_S=\frac{1}{3}\pi$ (°K)
1	12.5	335	313	299
2	18	341	331	323
3	21.5	308	309	311
4 (Bragg)	63	359	350	336

[a] Peak position used in determining effective Debye temperatures (position at 600°K).

of the bulk ions for a case in which the surface layer is vibronically inequivalent to the bulk layers. For the Bragg peak (4), increasing the scattering power of the surface ions relative to that of the bulk ions moves the effective Debye temperature towards that of the surface layer. The intralayer multiple-scattering peak 1 also exhibits this behavior. The split $n=2$ primary Bragg peak (i.e., peaks 2 and 3) does not exhibit a simple behavior.

In Table IV we show the effect of the electron inelastic-collision mean free path on the effective Debye temperature for a case in which the surface and bulk layers are both electronically and vibronically inequivalent. The calculation is performed for a surface layer which scatters more strongly than the bulk and also has a larger amplitude of vibration. As might be expected, for the Bragg peak decreasing the electron mean free path enhances the influence of the surface layer. This also occurs in the case of the split $n=2$ primary Bragg peak but not for the intralayer multiple-scattering peak 1.

It appears in general that the "simple" Bragg peaks respond in the expected manner to variation of the parameters of the system but that the intralayer multiple-scattering peak and the components of the split $n=2$ Bragg peak behave in no set way. It also appears that the effective Debye temperatures not only depend on the vibrational amplitudes of the surface and bulk ions but also depend quite sensitively on the inelastic-collision mean free path and on the relative scattering power of the surface and bulk ions. Therefore, the model does not seem to provide a diagnostic tool for distinguishing between the electronic and the vibronic inequivalence of the bulk and surface layers. Although such a situation is not desirable, it is predictable from the fact that the effective ion-core scattering amplitudes, the $b_\lambda(\mathbf{k}_f, \mathbf{k}_i; E)$ defined by Eq. (5), contain the product of the electronic vertex $t_\lambda(\mathbf{k}_f, \mathbf{k}_i; E)$ and the phonon renormalization factor $\exp[-W_\lambda(\mathbf{k}_f-\mathbf{k}_i)]$. In principle, the electronic factor can be determined in part by analyzing low-temperature data for which W_λ becomes independent of the temperature [see, e.g., Eq. (61)]. However, even in this limit the theory clearly predicts that the consequences of the electronic scattering properties of the ion-core potentials are inextricably intermixed with those of the zero-point motion of the ions. Only for low-energy scattering from heavy ion cores (i.e., $W_\lambda\to 0$) does the electron-solid scattering cross section depend solely on the individual electron–ion-core potentials.

V. SUMMARY AND CONCLUSIONS

We took as our starting point for this paper a set of integral equations[12] describing the elastic scattering cross section for low-energy electron scattering from a vibrating lattice. In this paper we discussed the reduction of these integrals to a set of algebraic equations with subject only to some general assumptions about the form of the ion core potential seen by the electrons. We then investigated the predictions of these equations using a very simple model of the solid—taking only s-wave scattering to describe the electronic interaction with a rigid-ion core using the Debye model for the phonon spectrum of the solid. Specifically, we chose the parameters of the calculation to correspond to electrons scattering from Al(100). Our main conclusions can be summarized as follows:

(i) The effective single-site scattering vertex consists of the rigid-ion scattering vertex multiplied by a "Debye-Waller" factor. The Debye-Waller factor can introduce a significant amount of higher partial waves into the calculation. It also renders ambiguous the distinction between "electronic" and "vibronic" effects.

(ii) Thermal lattice expansion can significantly shift the positions of the peaks in the elastic energy profile, but it has negligible effect on their heights.

(iii) Thermal lattice vibration can change not only the over-all height of an energy profile, but can also change the relative heights of peaks within an energy profile.

(iv) The temperature dependence of both Bragg peaks and intralayer multiple-scattering peaks can be

TABLE IV. Influence of inelastic-collision mean free path on the effective Debye temperature for a vibronically and electronically inequivalent surface layer of ion-core potentials. Parameters of the calculation: $\Theta_D{}^B=426°\text{K}$, $\Theta_D{}^S=300°\text{K}$, $\delta_B=\frac{1}{5}\pi$, $\delta_S=\frac{1}{3}\pi$.

Peak	Energy[a] (eV)	$\lambda_{ee}=15$ Å (°K)	$\lambda_{ee}=10$ Å (°K)	$\lambda_{ee}=6$ Å (°K)
1	12.5	299	299	321
2	18	395	323	297
3	21.5	322	311	303
4 (Bragg)	63	362	336	311

[a] Peak position used in determining effective Debye temperatures (position at 600°K).

characterized quite well by an effective Debye temperature obtained from a "Born-approximation" (kinematical) analysis. However, the dependence of these effective Debye temperatures upon the parameters of the material can be quite different for peaks with differing dynamical origins.

(v) The effective Debye temperatures obtained from a kinematical analysis of intensity profiles do not depend solely on the vibrational amplitudes of the surface and the bulk ions. They also depend sensitively on the scattering power of the surface ions relative to the bulk ions and the effective penetration of the electron beam into the solid.

(vi) Because of point (v) we conclude that one can utilize the conventional "Born-approximation" analysis of the temperature dependence of the low-energy Bragg peaks to obtain reliable semiquantitative information about the vibrational amplitudes of the surface ions, only if independent determination both of the difference in the scattering of surface and bulk ion cores and of the inelastic-collision damping of the incident beam are available.

Finally, we recall that we can speak of "primary" and "secondary" Bragg peaks only because we are using a finite-order perturbation-theory solution to the equations for the scattering amplitudes.[4] In the case of a complete matrix-inversion analysis, the kinematical "Bragg" condition usually is reflected in the intensity profiles as an envelope function for the intensity of various multiple-scattering peaks.[3–5] Therefore unless the electron–ion-core scattering amplitudes are small,[5] we anticipate that a matrix inversion analysis will enhance further the difficulties in semiquantitative data analysis described in conclusions (i), (iv), (v), and (vi) above.

---

* Work supported in part by the Advanced Research Project Agency under Contract No. SD-131.

† NSF Postdoctoral Fellow.

[1] C. B. Duke and C. W. Tucker, Jr., Surface Sci. **15,** 231 (1969).

[2] R. O. Jones and J. A. Strozier, Jr., Phys. Rev. Letters **22,** 1186 (1969).

[3] C. B. Duke and C. W. Tucker, Jr., Phys. Rev. Letters **23,** 1163 (1969).

[4] C. B. Duke, J. R. Anderson, and C. W. Tucker, Jr., Surface Sci. **19,** 117 (1970).

[5] C. W. Tucker, Jr. and C. B. Duke, Surface Sci. (to be published).

[6] B. W. Holland, R. W. Hannum, and A. M. Gibbons, Surface Sci. (to be published).

[7] W. H. Weber and M. B. Webb, Phys. Rev. **177,** 1103 (1969).

[8] J. I. Gersten, Phys. Rev. **188,** 774 (1969).

[9] C. B. Duke, G. E. Laramore, and V. Metze, Solid State Commun. **8,** 1189 (1970).

[10] C. B. Duke and G. E. Laramore, in Proceedings of the Thirtieth Annual Conference on Physical Electronics, 1970, paper No. C7 (unpublished); in Proceedings of the Fourth LEED Theory Seminar, 1970, pp. 10–17 (unpublished).

[11] Y. H. Ohtsuki, J. Phys. Soc. Japan **29,** 398 (1970).

[12] C. B. Duke and G. E. Laramore, preceding paper, Phys. Rev. B **2,** 4765 (1970).

[13] M. Born, Rept. Progr. Phys. **9,** 294 (1942).

[14] C. Kittel, *Quantum Theory of Solids* (Wiley, New York, 1963), Chap. 19.

[15] H. Yoshioka and Y. Kainuma, J. Phys. Soc. Japan **17,** 134 (1962).

[16] R. F. Wallis and A. A. Maradudin, Phys. Rev. **148,** 962 (1966).

[17] D. L. Mills, J. Phys. Chem. Solids **28,** 2245 (1967).

[18] R. E. DeWames and L. A. Vredovoe, Phys. Rev. Letters **18,** 853 (1967).

[19] J. T. McKinney, E. R. Jones, and M. B. Webb, Phys. Rev. **160,** 523 (1967).

[20] R. F. Barnes, M. G. Lagally, and M. B. Webb, Phys. Rev. **171,** 627 (1968).

[21] (a) See, for example, I. H. Kyan, J. P. Hobson, and R. A. Armstrong, Phys. Rev. **129,** 1513 (1963); G. Gafner, Surface Sci. **19,** 9 (1970). (b) R. Baudoing, C. Corotte, and A. Mascall, J. Phys. Colloq. **31,** Cl-21 (1970).

[22] A. U. McRae and L. H. Germer, Phys. Rev. Letters **8,** 489 (1962).

[23] A. U. McRae, Surface Sci. **2,** 522 (1964).

[24] E. R. Jones, J. T. McKinney, and M. B. Webb, Phys. Rev. **151,** 476 (1966).

[25] R. M. Goodman, H. H. Farrell, and G. A. Somorjai, J. Chem. Phys. **48,** 1046 (1968).

[26] J. M. Morabito, Jr., R. F. Steiger, and G. A. Somorjai, Phys. Rev. **179,** 638 (1969).

[27] J. L. Beeby, J. Phys. C **1,** 82 (1968).

[28] See, for example, J. D. Jackson, *Classical Electrodynamics* (Wiley, New York, 1963), Chap. 3.

[29] C. Kittel, *Introduction to Solid State Physics* (Wiley, New York, 1963), Chap. 6.

[30] A. A. Maradudin, E. W. Montroll, and G. H. Weiss, in *Solid State Physics,* edited by F. Seitz and D. Turnbull (Academic, New York, 1963), Suppl. 3.

[31] W. A. Harrison, *Pseudopotentials in the Theory of Metals* (Benjamin, New York, 1966).

[32] M. L. Goldberger and K. M. Watson, *Collision Theory* (Wiley, New York, 1964), Chap. 6.

[33] H. A. Antosiewicz, Natl. Bur. Std. (U.S.) Appl. Math. Ser. **55,** 435 (1964).

[34] The sum over L_3 involves only a finite number of terms for fixed L_1 and L_2. This is because $I(L_1; L_2, L_3)$ is nonzero only for $|l_2-l_3| \leq l_1 \leq l_2+l_3$. See, for example, M. E. Rose, *Elementary Theory of Angular Momentum* (Wiley, New York, 1957), p. 62.

[35] We use the measured thermal expansion coefficient for bulk aluminum to determine the change of the lattice constant with temperature. See A. Goldsmith, T. E. Waterman, and H. J. Hirschhorn, *Handbook of Thermophysical Properties of Solid Materials* (MacMillan, New York, 1961), Vol. I, p. 49.

[36] C. B. Duke, J. Vac. Sci. Technol. **6,** 152 (1969).

[37] E. Bauer, J. Vac. Sci. Technol. **7,** 3 (1970).

[38] D. P. Woodruff and M. P. Seah, Phys. Letters **30A,** 263 (1969).

[39] This fact has recently been observed experimentally as well: C. D. Gelatt, Jr., M. G. Lagally, and M. B. Webb, Bull. Am. Phys. Soc. **15,** 632 (1970).